Rapid Prototyping of a Low-Cost Solar Array Simulator Using an Off-the-Shelf DC Power Supply

Article *in* IEEE Transactions on Power Electronics · October 2014

DOI: 10.1109/TPEL.2013.2291837

3 authors:

Shlomo Gadelovits
The University of Sheffield
11 PUBLICATIONS **76** CITATIONS
SEE PROFILE

Moshe Sitbon
Ariel University
26 PUBLICATIONS **180** CITATIONS
SEE PROFILE

Alon Kuperman
Ben-Gurion University of the Negev
159 PUBLICATIONS **2,022** CITATIONS
SEE PROFILE

Rapid Prototyping of a Low Cost Solar Array Simulator Using an Off-the-Shelf DC Power Supply

S. Gadelovits, *Student Member, IEEE*, M. Sitbon, *Student Member, IEEE* and A. Kuperman, *Member, IEEE*

***Abstract*— A method of rapid prototyping of a Solar Array Simulator, based on low cost, off-the-shelf components is proposed in the paper. A commercial constant output voltage switching power supply is utilized as a power stage. It is shown that it is possible to gain control over output voltage of such a device by injecting variable analog voltage into the voltage feedback loop of the supply. As a result, by sensing the power supply output current and varying the injected voltage it is possible to change the output voltage according to a predefined relation and hence any static I-V curve may be emulated by the device. For simulating a solar array output characteristics, the desired I-V curve may be either digitized from a manufacturer provided datasheet, obtained experimentally or estimated from three basic current-voltage pairs (open circuit, short circuit and maximum power points) using a dedicated algorithm. In order to demonstrate the proposed method, a prototype was designed and built based on available low-cost commercial components. Dynamic characteristics of the prototype were experimentally evaluated and three static I-V curves of a commercial solar panel were simulated. The resulting I-V output characteristics were shown to closely resemble datasheet I-V curves.**

***Index Terms*— Solar array simulator, Rapid prototyping, Low cost, Digital Signal Processor.**

I. Introduction

ELECTRICITY generation based on renewable (e.g. photovoltaic, wind etc.) and alternative (e.g. fuel cell etc.) energy generators both on low and high power levels has gained an enormous popularity during the last decades. While breaking the dependence on the conventional fossil fuels, such generators possess highly nonlinear output characteristics, strongly influenced by environmental operating conditions (temperature, solar irradiation, wind speed, altitude etc.) and should be interfaced with special care typically either by a power converter, implementing a Maximum Power Point Tracking (MPPT) algorithm [1] or a properly matched load [2]. As a result, such energy generators operation should be judiciously evaluated prior to deployment through the whole possible operating range. In order to evaluate the performance of the selected interfacing method, a hardware simulator is usually employed during the prototyping phase, allowing (in addition to normal operation) to both push the system to its boundary conditions and create faulty scenarios without damaging the actual generator. While solar array simulators (SAS) are probably the most common [3-7], wind turbine [8, 9] and fuel cell [10, 11] simulators have been widely used as well. Apart of the reasons listed above, SAS is particularly useful when solar array performance should be recreated under currently unachievable environmental conditions such as extraterrestrial solar irradiation, cold temperature in hot climate conditions and vice versa [12-14]. Performance under partial shading is also considered a major issue in photovoltaic generation and several simulators were designed to evaluate its effect on energy production [15-17].

Currently, the main commercial SAS drawback is the high price, making the device almost impossible to have for an average educational laboratory or even a small company. This is the why custom solar array simulators have been widely proposed in the literature since the first programmable prototype in the late 60's [18]. While the most advanced custom solar array simulators contain digital programmable hardware, several simple fully analog devices were proposed in case where only limited amount of I-V curves was required to be simulated [19, 20]. Low cost designs were described in [21, 22].

In most cases found in the literature, custom SAS are created from scratch, i.e. both the power and control circuits are designed and built [23-26]. Obviously, the deployment time of such prototypes is relatively high. In this paper, a rapid prototyping method of a low-cost custom SAS design is proposed. Instead of designing the controlled power stage from scratch, an off the shelf constant output voltage power supply is utilized. Such supplies are widely available on the market, low cost and robust, mainly used to create stable supply voltages (e.g. 12V, 5V, 3.3V etc.). The main drawback of these devices is the fact that their output voltage tracks fixed reference voltage, internally created by the control IC and thus inaccessible. In order to emulate an I-V curve, SAS must be able to vary its output voltage. Hence, a method of gaining fast control over the output voltage of an off the shelf constant output voltage power supply is demonstrated in the paper, allowing to utilize such devices in any I-V curve simulator. The proposed method could also be used in order to emulate and test PV systems adopting the so distributed maximum power point tracking (DMPPT) architectures. In particular, instead of emulating the static characteristics of single PV modules, it could be possible to emulate static characteristics

The authors are with the Hybrid Energy Sources R&D Laboratory, Ariel University, Dept. of Electrical Engineering and Electronics, Ariel 40700, Israel (Tel. +972-526943234; fax: +97239066238, email: alonku@ariel.ac.il).

of systems composed by PV modules equipped with their own MPPT converters [27]. This could be very useful in order to test the performances (advantages and drawbacks) of various DMPPT architectures.

It is important to note that that rather than presenting a novel approach to implement a solar simulator using a particular topology, the paper focuses on rapidly constructing one based on any off-the-shelf constant output voltage converter (not necessarily a dc-dc one). The proposed approach is in no way limited to any particular topology.

The rest of the manuscript is arranged as follows. Section II reveals the structure of a typical SAS and its modes of operation, followed by principle and limitation of an off-the-shelf power supply operation revised in Section III. Modification necessary to gain fast control over the off-the-shelf power supply output voltage allowing arbitrary I-V curve emulation is derived in Section IV. Experimental prototype is demonstrated and discussed in Section V, followed by the manuscript conclusions in Section VI.

II. Typical SAS Structure and Modes of Operation

Solar array simulators are usually available is either standalone or PC-controlled configuration. Typical SAS consists of a conventional power stage and application specific software module, as shown in Fig. 1. The power stage is usually an off-grid single or three phase power supply (depending on the power rating), formed by an AC/DC front end and a DC/DC converter. Generally, in case DC input is available, only DC/DC converter is necessary since the AC/DC stage does not take part in the I-V curve emulation. Note that since the hardware part of a SAS is a conventional power supply, any SAS may operate in a pure power supply mode (also referred to as *FIXED* mode), implementing a rectangular I-V characteristics of a current limited voltage source, i.e. the reference voltage v_{REF} in Fig. 1 is directly set by the user. This mode is of no interest here and will not be further discussed.

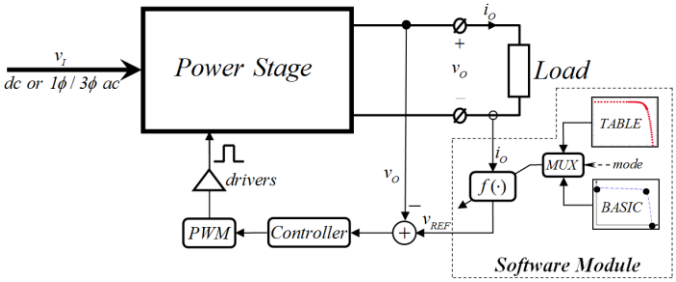

Fig. 1. Typical SAS structure

The two relevant modes of operation are *BASIC* and *TABLE* modes, realized either in PC software or embedded in SAS in case of a standalone device. In the *BASIC* mode, three reference points (short-circuit current, open-circuit voltage and MPP current and voltage) are provided to the simulator and the device estimates the remaining I-V curve points using a predefined algorithm for arbitrary weather conditions, requested by the user. The irradiance and temperature variations may be performed manually in real time, supplied as predefined time-dependent vectors, or alternatively chosen from recorded data files, usually supplied with SAS.

In the *TABLE* mode, the desired I–V curve represented by a vector of voltage–current pairs is fed into the device. The device then uses interpolation to realize a quasi-continuous I-V curve. It is worth noting that when operating in this mode, SAS may follow any I-V curve (within operational limits), emulating e.g. fuel cell, battery etc.

The trade-off between the two mentioned operating modes is as follows. The *BASIC* mode allows emulating solar panels with minimum available data at the expense of reproduction accuracy. On the other hand, as noticed in [28], in order to reproduce PV generator characteristics with the highest precision, the SAS should operate in *TABLE* mode, requiring as many as possible voltage-current pairs, either extracted from a detailed datasheet of obtained experimentally.

When a mode is selected and the desired environmental conditions are set, SAS operates as follows. An emulated I-V curve is calculated by the software module, the SAS output current is sensed and the appropriate voltage reference signal is sent to the power stage. The power supply voltage loop bandwidth (typically up to 1 kHz) should then be much higher than the rate of environmental conditions variations (which is usually relatively low, dominated by the irradiance bandwidth of up to 1-2 Hz). Moreover, if SAS is loaded by a power converter implementing a MPPT algorithm, its bandwidth should be at least 5-8 times lower (as a rule of thumb) than the SAS voltage loop bandwidth in order to obtain accurate results. In case of environmental conditions change, the software module re-calculates the I-V curve and the voltage reference signal sent to the power stage is updated accordingly.

III. Off-the-shelf Power Supply Principle of Operation and Limitations

A typical off the shelf commercial DC power supply is shown in Fig. 2. The main goal of the device is regulating the output voltage to a predefined value despite input voltage variations for a variety of loads. The system usually contains a power stage and a control IC.

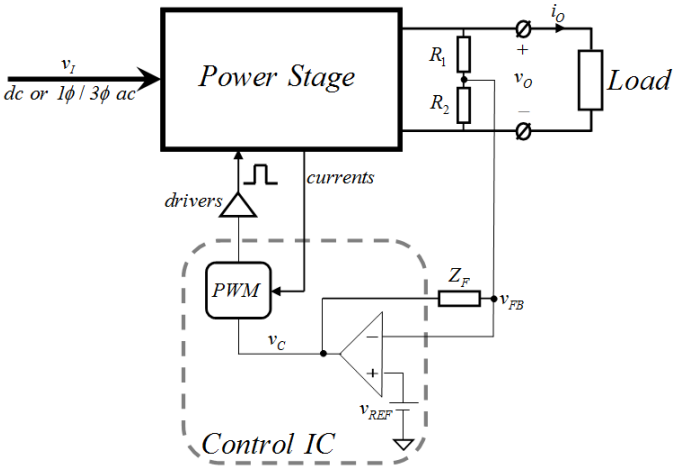

Fig. 2. Typical off-the-shelf commercial power supply

The load voltage is usually sensed by a voltage divider and fed into the control IC. Switch/inductor currents are typically sensed as well in order to either perform a cycle-by-cycle

current limitation or implement an inner current control loop. The voltage loop is typically implemented by means of an error amplifier with an external analog compensation network Z_F. The feedback voltage $v_{FB} = v_O \cdot R_2 \cdot (R_1+R_2)^{-1}$ is compared to a fixed internal reference v_{REF} and the control signal v_C is supplied to a PWM generating unit. In steady state, $v_{FB} = v_{REF}$, hence the output voltage is regulated to

$$v_O = (1+\frac{R_1}{R_2})v_{REF} . \quad (1)$$

Such circuits are widely used to create a variety of supply voltages (e.g. 3.3V, 5V, 12V etc.). While simple and robust, the structure of such power supplies does not allow dynamic changes of their output voltage since the voltage reference is fixed and resides inside the control IC. If it is desired to manually vary the output voltage, one of the voltage divider resistors may be replaced by a potentiometer. Nevertheless, since there is no direct access to v_{REF} it is impossible to directly implement the SAS structure shown in Fig. 1 using such a power supply without modifications since it requires fast controlled voltage tracking.

From the control point of view, the block diagram of a closed loop controlled DC power supply is shown in Fig. 3, where $C(s)$ is the error amplifier network transfer function, $\mathbf{P}(s)$ is the 1x3 plant transfer function matrix and $k = R_2 \cdot (R_1+R_2)^{-1}$. As mentioned above, the main goal is regulating v_O to v_{REF} despite input voltage v_I and load i_O variations.

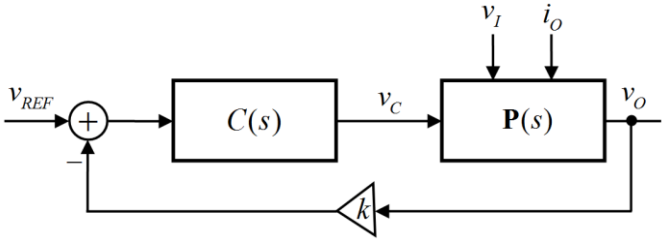

Fig. 3. Voltage loop of a commercial power supply

In frequency domain, the output voltage is given by

$$v_O(s) = H_{rv}(s) \cdot v_{REF}(s) + H_{vv}(s) \cdot v_I(s) + H_{iv}(s) \cdot i_O(s) , \quad (2)$$

where $H_{rv}(s)$, $H_{vv}(s)$ and $H_{iv}(s)$ are reference-to-output, input-to-output and load-to-output transfer functions, respectively, hence if the loop is compensated correctly, $|H_{rv}(\omega)| \to 1$, $|H_{vv}(\omega)| \to 0$ and $|H_{iv}(\omega)| \to 0$ for $0 < \omega < \omega_V$ with ω_V being the voltage controller crossover frequency. Typical ω_V depends on the power stage topology and is limited by several kHz in boost and buck-boost derived topologies and by several tens of kHz in buck derived topologies.

IV. Power Supply Modification to Gain Fast Control over Output Voltage

Consider an off-the-shelf commercial power supply shown in Fig. 2 with the following modification: an external controlled voltage source v_X is connected to the point of connection of the feedback resistors R_1 and R_2, as shown in Fig. 4.

The feedback voltage is now given by

$$v_{FB} = \frac{R_2 \parallel R_3}{R_1 + R_2 \parallel R_3} v_O + \frac{R_1 \parallel R_2}{R_3 + R_1 \parallel R_2} v_X \quad (3)$$

and since in steady state v_{FB} is still equal to v_{REF}, the output voltage is now regulated to

$$v_O = \left(1+\frac{R_1}{R_2 \parallel R_3}\right)\left(v_{REF} - \frac{R_1 \parallel R_2}{R_3 + R_1 \parallel R_2} v_X\right) = \left(1+\frac{R_1}{R_2 \parallel R_3}\right) v_{REF_M} . \quad (4)$$

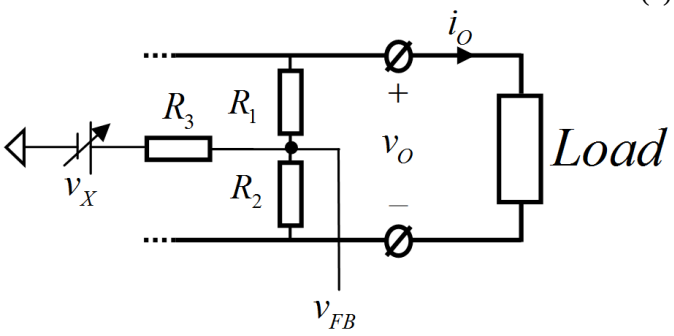

Fig. 4. Commercial power supply modification

From the control point of view, the block diagram of a modified closed loop controlled DC power supply is shown in Fig. 5 with $k_1 = R_2||R_3 \cdot (R_1 + R_2||R_3)^{-1}$ and $k_2 = R_1||R_2 \cdot (R_3 + R_1||R_2)^{-1}$. In frequency domain the output voltage is now given by

$$v_O(s) = H_{rv}(s) \cdot v_{REF_M}(s) + H_{vv}(s) \cdot v_I(s) + H_{iv}(s) \cdot i_O(s) , \quad (5)$$

with k substituted by k_1. Since the injection of v_X does not affect the loop gain an important observation should be pointed out: $|H_{rv}(\omega)| \to 1$, $|H_{vv}(\omega)| \to 0$ and $|H_{iv}(\omega)| \to 0$ for $0 < \omega < \omega_V$ still hold, i.e. disturbance rejection and tracking capabilities are unaffected by the modification. Hence, by performing the suggested modification fast control over the power supply output voltage may be attained without sacrificing the disturbance rejection. In order to regulate the power supply output voltage to V, the injected voltage should be

$$v_X = \left(1+\frac{R_3}{R_1 \parallel R_2}\right)\left(v_{REF} - \frac{R_2 \parallel R_3}{R_1 + R_2 \parallel R_3} V\right) \quad (6)$$

according to (4).

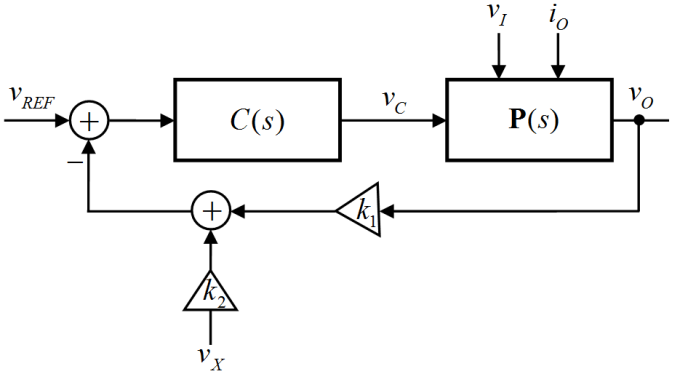

Fig. 5. Modified voltage loop of a commercial power supply (open loop control)

It is important to note that since v_{REF} is constant, the dynamics of v_O is now entirely driven by the injected voltage v_X. Therefore in order to obtain good tracking, the bandwidth of v_X should be (as a rule of thumb) at least 5-8 times lower than ω_V.

In order to emulate an I-V curve of a solar panel, the SAS must be capable of sensing currents in the range of $0 < i_O <$

$I_{SC,MAX}$ (maximum short circuit current is expected in case of highest irradiance and temperature) and creating voltages in the range of $V_{OC,MAX} > v_O > 0$ (maximum open circuit voltage is expected in case of highest irradiance and lowest temperature). Note that the injected voltage will usually be limited, $v_{X,MIN} < v_X < v_{X,MAX}$. Rewriting (4) as

$$v_O = k_1^{-1}\left(v_{REF} - k_2 v_X\right) \tag{7}$$

and plotting in Fig. 6 leads to the following constraints on selecting k_1 and k_2 (and hence resistors R_1, R_2 and R_3),

$$\begin{cases} k_2^{-1} v_{REF} \le v_{X,MAX} \\ k_1^{-1}\left(v_{REF} - k_2 v_{X,MIN}\right) \ge v_{OC,MAX} \end{cases}. \tag{8}$$

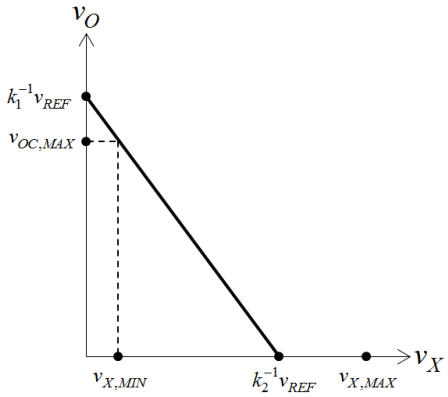

Fig. 6. Deriving resistors selection constraints

In case both constraints are satisfied, the short circuit conditions (v_O = 0) are achieved by setting $v_X = k_2^{-1} v_{REF}$. In order to realize the open circuit conditions (v_O = V_{OC}), the injected voltage must satisfy $v_X = k_2^{-1}\left(v_{REF} - k_1 V_{OC}\right)$. Moreover, if $v_{X,MIN}$ = 0, the open circuit voltage will be given by $V_{OC} = k_1^{-1} v_{REF}$.

V. Experiments and Discussion

In order to implement the presented method, a simple SAS prototype was built as shown in Fig. 7. A low cost (~15$) 100W DC-DC converter (buck topology) based power supply board was purchased on *Ebay*. The controller used in the power supply utilizes voltage control with pulse-by-pulse current limitation. The injected voltage v_X was realized by low-pass filtering of a high frequency PWM signal (1-bit D/A), created by a TMS320F28335 Digital Signal Processor and connected to the feedback node of the power supply via an additional resistor. The power supply output current was sensed by the DSP via a shunt resistor followed by an amplifier. The required I-V curves were fed into the DSP from a PC using Labview software via RS-232 port. The PC software was designed to operate the prototype in *TABLE* mode. The power supply board was fed from a laboratory DC source and connected to an NHR-4700 programmable DC load. The SAS prototype is pictured in Fig. 8.

The relevant system parameter values are summarized in Table I. Internal reference voltage of the control IC was estimated by measuring the voltage of the feedback node in steady state prior to the power supply board modification. Since the voltage v_X was created by low pass filtering of the DSP PWM signal, it is bounded by DSP voltage levels (0V and 3.3V). The resistors values were chosen in order to satisfy (8) while allowing creating voltages from 0V (attainable at v_X = 1.64V) up to 36V (attainable at v_X = 0).

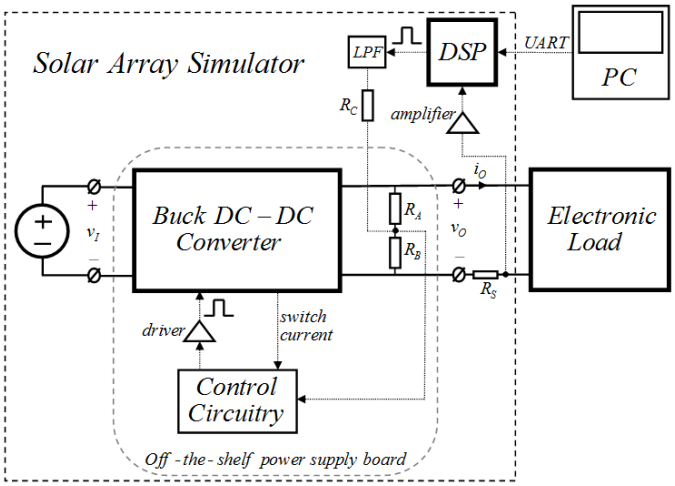

Fig. 7. Block diagram of SAS prototype-based system

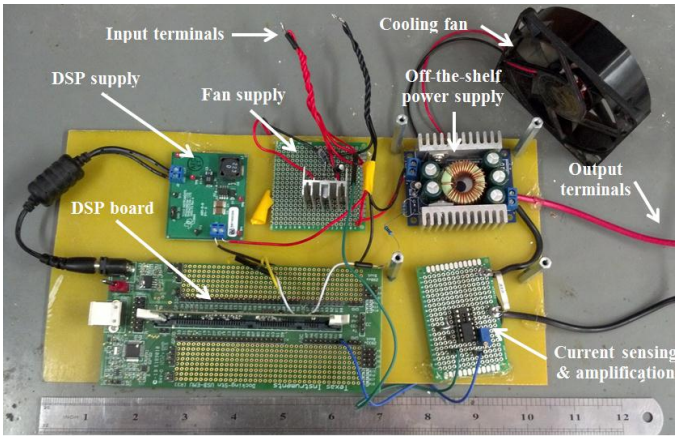

Fig. 8. Picture of the SAS prototype

TABLE I: System Parameter Values

Parameter	Value	Units
v_{REF}	0.8	[V]
R_A	220	[kΩ]
R_B	10	[kΩ]
R_C	10	[kΩ]
$v_{X,MIN}$	0	[V]
$v_{X,MAX}$	3.3	[V]

In order to estimate the voltage loop bandwidth of the off-the-shelf power supply board, step changes of v_X between 0.2 V to 0.9 V were applied to the system, as shown in Fig. 9 along with the SAS output voltage response. According to (4) and taking into account the system parameters in Table I, the SAS output voltage should be fluctuating between 28.2 V and 16.2 V. This is supported by the experimental results in Fig. 9. Note that the voltage transient time is about 20 ms, i.e. the voltage loop bandwidth is around 50 Hz. Therefore such a

device may be employed for evaluating MPPT algorithms with bandwidths up to 10 Hz.

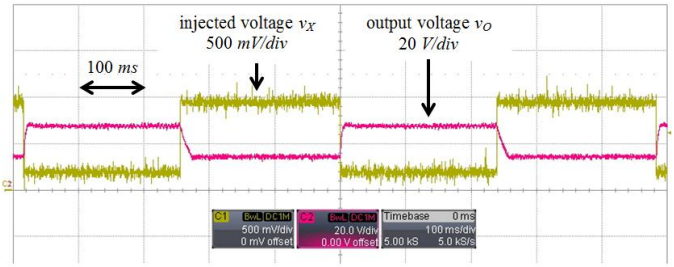

Fig. 9. Voltage loop bandwidth estimation results

In order to evaluate the ability of SAS prototype to follow static I-V curves, the device was programmed to simulate a 50W Lorenz LC50-12M solar panel. The manufacturer provided I-V curves of the array for different irradiation levels and temperatures are shown in Fig. 10. Three of the curves (1 – 1000W·m^{-1} / 25^{o}C, 2 – 400 W·m^{-1} / 25^{o}C, 3 – 1000W·m^{-1} / 50^{o}C) were first digitized from the datasheet using dedicated software and recorded into an Excel file. The PC then transferred the selected curve to the DSP which performed the solar panel emulation according to the flowchart in Fig. 11 as follows. The DSP receives the I-V curve vector via the Serial Communication Interface (SCI) and stores it into a look-up table (LUT) after appropriate scaling. The power supply output current is sensed by an Analog-to-Digital Converter (ADC) and fed into the look-up table after scaling. Since the proposed method is actually open-loop (there is no voltage feedback to DSP), slight drifts occur during the operation because of resistor/capacitor values tolerances, wiring/soldering resistances not taken into account, quantization errors etc. These inaccuracies were measured offline and found to be systematic, depending mostly on the output current. After several experiments, this dependence was quantified and appropriate feed-forward error correction (FEC) term was created and added to the LUT output to offset the drifts. The injected voltage creating PWM signal was formed by summing and scaling the LUT output and the correcting term.

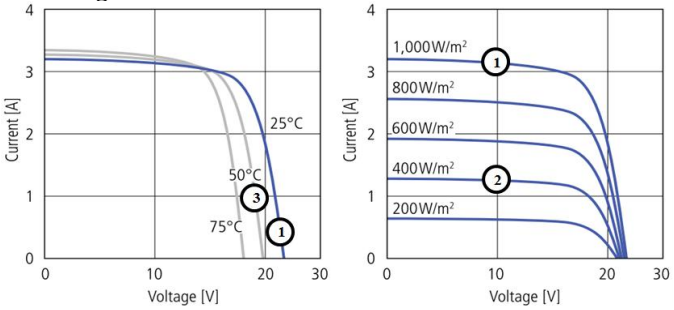

Fig. 10. Lorenz LC50-12M array I-V curves for different temperatures at constant irradiation of 1000W·m^{-2} (left) and different irradiation levels at constant temperature of 25^{o}C (right)

Static SAS behavior results are shown in Figs. 12 – 14. It may be concluded that the emulated I – V curves are closely followed and the small errors may be considered satisfactory for such a simple, open loop controlled rapid prototype. As expected, the accuracy near the open circuit condition is the highest and deteriorates towards the short circuit point because of reduced system stability [29].

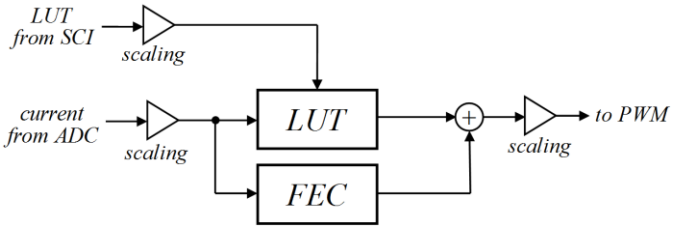

Fig. 11. DSP software flowchart

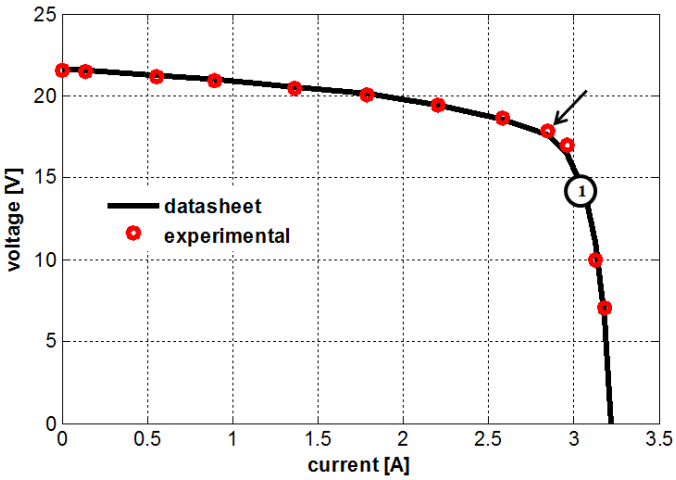

Fig. 12. Datasheet versus SAS created I-V curve for 1000W·m^{-2} / 25^{o}C

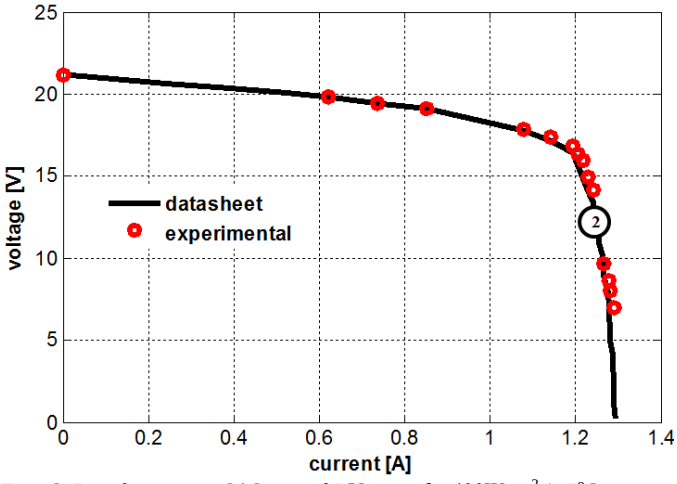

Fig. 13. Datasheet versus SAS created I-V curve for 400W·m^{-2} / 25^{o}C

In order to demonstrate SAS dynamic performance, the system was first set to follow the 50W Lorenz LC50-12M solar panel I-V curve for 1000W·m^{-2} / 25^{o}C, as shown in Fig. 12. Next, a 6.5 Ω resistor was connected to the SAS output and then removed after nearly 80 ms. The results are shown in Fig. 15. Prior to the load connection, SAS operates in an open circuit mode with $v_O \approx 22$ V. After the load application, SAS settles at panel maximum power point (~18 V, ~2.8 A), shown with black arrow in Fig. 12. When the load is removed, SAS returns to the open circuit mode.

Three points should be emphasized. First, it is possible to reduce the steady state error to near-zero by feeding the output voltage to DSP and closing the loop as shown in Fig. 16,

where the output current is sampled and fed into a LUT, creating a reference output voltage signal v_O^{REF}. The reference output voltage signal is then compared to sampled actual output voltage and the error is processes by a selected controller, creating the control voltage v_X. Nevertheless, adding an extra loop would slow down the SAS operation in terms of allowable MPPT bandwidth since the output voltage control performed by the DSP must not interfere with the voltage control of the power supply and thus its bandwidth should be at least five times lower.

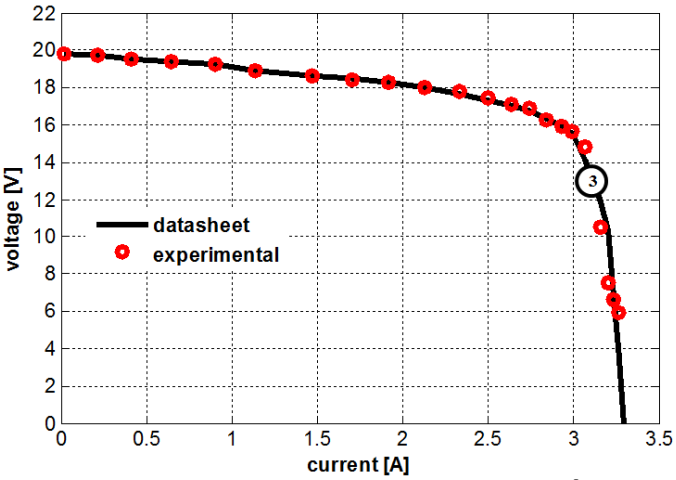

Fig. 14. Datasheet versus SAS created I-V curve for 1000W·m^{-2} / 50°C

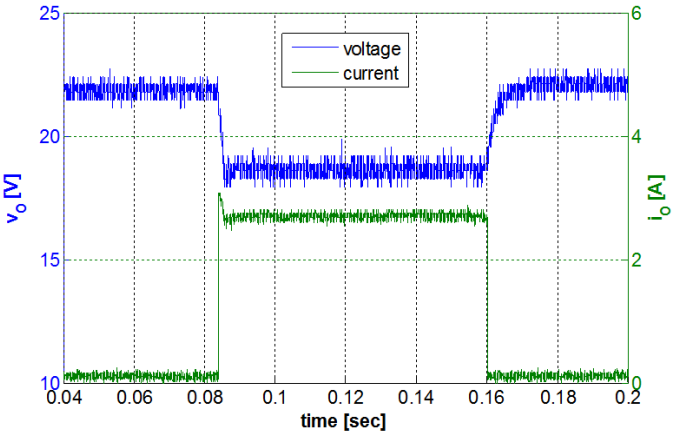

Fig. 15. Dynamic behavior experimental results

Second, while the presented prototype was designed to operate in *TABLE* mode, it can easily be extended to *BASIC* mode by implementing one of the algorithms available in the literature (see [30] - [32] for more information). The point is that when the device operates in *SAS* mode, it estimates I-V curves instead of obtaining them from the user. Once an I-V curve is estimated, the remaining process is the same as presented above.

Third, the main controller was implemented using a relatively expensive TMS320F28335 based control card just for convenience. Since the controller executes a simple routine, it may be easily implemented on any low-cost platform e.g. Arduino or MSP430 thus reducing the overall cost.

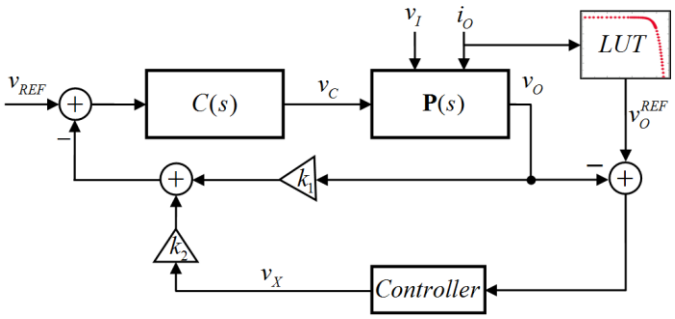

Fig. 16. Modified voltage loop of a commercial power supply (closed loop control)

VI. Conclusion

A method of rapid prototyping of a Solar Array Simulator, based on a low cost, off-the-shelf constant output voltage power supply was presented in the paper. It was shown that it is possible to gain control over output voltage of such a device by injecting control voltage into the voltage feedback node. Hence, by sensing the power supply output current and changing the output voltage according to a predefined relation, any static I-V curve may be emulated. For simulation of a solar array, the desired I-V curve may be either digitized from a manufacturer provided datasheet, obtained experimentally or estimated from the three basic current-voltage pairs (open circuit, short circuit and MPP) using a dedicated algorithm. Since the control voltage is bounded in magnitude, several constraints regarding the feedback network selection based on the desired output I-V characteristics must be satisfied. A prototype was designed and built based on available commercial components. The dynamic characteristics of the prototype were evaluated and three static I-V curves of a commercial solar panel were simulated. The resulting SAS I-V output characteristics closely resembled the datasheet I-V curves. It was concluded that it is possible to reduce the steady state error by realizing an additional voltage loop at the expense of attainable SAS bandwidth.

VII. References

[1] B. Subudhi and R. Pradhan, "A comparative study on maximum power point tracking techniques for photovoltaic systems," *IEEE Transactions on Sustainable Energy*, vol. 4, no. 1, January 2013.

[2] A. Kuperman, M. Averbukh and S. Lineykin, "Maximum power point matching versus maximum power point tracking for solar generators," *Renewable and Sustainable Energy Reviews*, vol. 19, pp. 11-17, 2013.

[3] A. Mellit, H. Mekki, A. Messai and H. Salhi, "FPGA-based implementation of an intelligent simulator for stand-alone photovoltaic system," *Expert Systems with Applications*, vol. 37, pp. 6036-6051, 2010.

[4] M. Park and I.-K. Yu, "A novel real-time simulation technique of photovoltaic generation systems using RTDS," *IEEE Transactions on Energy Conversion*, vol. 19, no. 1, pp. 164-169, March 2004.

[5] Y. Kim, W. Lee, M. Pedram and N. Chang, "Dual-mode power regulator for photovoltaic module emulation," *Applied Energy*, vol. 101, pp. 730-739, 2013.

[6] E. Koutroulis, K. Kalaitzakis and V. Tzitzilonis, "Development of an FPGA-based system for real-time simulation of photovoltaic modules," *Microelectronics Journal*, vol. 40, pp. 1094-1102, 2009.

[7] H. Matsukawa, K. Koshiishi, H. Koizumi, K. Kurokawa, M. Hamada and L. Bo, "Dynamic evaluation of maximum power point tracking with PV array simulator," *Solar Energy Materials and Solar Cells*, vol. 75, pp. 537-546, 2003.

[8] H. Kojabadi, L. Chang and T. Boutot, "Development of a novel wind turbine simulator for wind energy conversion systems using an inverter-

controlled induction motor," *IEEE Transactions on Energy Conversion*, vol. 19, no. 3, pp. 547-553, September 2004.
[9] M. Monfared, H. Kojabadi and H. Rastegar, "Static and dynamic wind turbine simulator using a converter controlled dc motor," *Renewable Energy* , vol. 33, pp. 906-913, 2008.
[10] J.-H. Jung, S. Ahmed and P. Enjeti, "PEM fuel cell stack model development for real-time simulation applications," *IEEE Transactions on Industrial Electronics*, vol. 58, no. 9, pp. 4217-4231, September 2011.
[11] C. de Beer, P. Barendse and A. Khan, "Development of an HT PEM fuel cell emulator using a multiphase interleaved DC-DC converter topology," *IEEE Transactions on Power Electronics*, vol. 28, no. 3, pp. 1120-1131, March 2013.
[12] M. Villalva, J. Gazoli and E. Filho, "Comprehensive approach to modeling and simulation of photovoltaic arrays," *IEEE Transactions on Power Electronics*, vol. 24, no. 5, pp. 1198-1208, May 2009.
[13] F. Attivissimo, A. Di Nisio, M. Savino and M. Spadavecchia, "Uncertainty analysis in photovoltaic cell parameter estimation," *IEEE Transactions on Istrumentation and Measurement*, vol. 61, no. 5, pp. 1334-1342, May 2012.
[14] L. Cristaldi M. Faifer, M. Rossi and F. Ponci, "A simple photovoltaic panel model: Characterization procedure and evaluation of the role of environmental measurements," *IEEE Transactions on Istrumentation and Measurement*, vol. 61, no. 10, pp. 2632-2641, October 2012.
[15] C.-C. Chen, H.-C. Chang, C.-C. Kuo and C.-C. Lin "Programmable energy source emulator for photovoltaic panels considering partial shadow effect," *Energy*, vol. 54, pp. 174-183, 2013.
[16] C. Sánchez Reinoso, D. Milone and R. Buitrago, "Simulation of photovoltaic centrals with dynamic shading," *Applied Energy*, vol. 103, pp. 278-289, 2013.
[17] M. Di Piazza and G. Vitale, "Photovoltaic field emulation including dynamic and partial shadow conditions," *Applied Energy*, vol. 87, pp. 814-823, 2010.
[18] P. Marenholtz, "Programmable solar array simulator," *IEEE Transactions on Aerospace and Electronic Systems*, vol. AES-2, no. 6, pp. 104-107, Nov 1966.
[19] G. Vachtsvanos and K. Kalaitzakis, "A hybrid photovoltaic simulator for utility interactive studies," *IEEE Transactions on Energy Conversion*, vol. EC-2, no. 2, pp. 227-231, June 1987.
[20] H. Nagayoshi, "I-V curve simulation by multi-module simulator using I-V magnifier circuit," *Solar Energy Materials and Solar Cells*, vol. 82, pp. 159-167, 2004.
[21] D. Lu and Q. Nguyen, "A photovoltaic panel emulator using a buck-boost DC/DC converter and a low cost micro-controller," *Solar Energy*, vol. 86, pp. 1477-1454, 2012.
[22] R. González-Medina, I. Patrao, G. Garcerá and E. Figueres, "A low-cost photovoltaic emulator for static and dynamic evaluation of photovoltaic power converters and facilities," *Progress in Photovoltaics: Research and Applications*, To appear.
[23] A. Vijayakumari, A. Devarajan and N. Devarajan, "Design and development of a model-based hardware simulator for photovoltaic array," *Electrical Power and Energy Systems*, vol. 43, pp. 40-46, 2012.
[24] A. Mukerjee and N. Dasgupta, "DC power supply used as photovoltaic simulator for testing MPPT algorithms," *Renewable Energy* , vol. 32, pp. 587-592, 2007.
[25] A. Koran, K. Sano, R.-Y. Kim, J.-S. Lai, "Design of a photovoltaic simulator with a novel reference signal generator and two-stage LC output filter," *IEEE Transactions on Power Electronics*, vol. 25, no. 5, pp. 1331-1338, May 2010.
[26] C.-H. Chang, E.-C. Chang and H.-L. Cheng, "A high-efficiency solar array simulator implemented by an LLC resonant DC–DC converter," *IEEE Transactions on Power Electronics*, vol. 28, no. 6, pp. 3039-3046, June 2013.
[27] M. Vitelli, "On the necessity of joint adoption of both distributed maximum power point tracking and central maximum power point tracking in PV systems", *Progress in Photovoltaics: Research and Applications*, Wiley-Blackwell, DOI: 10.1002/PIP.2256, pp. 1-17, 1099-159X, 2012.
[28] L. Nousiainen, J. Puukko, A. Maki, T. Messo, J. Huusari, J. Jokipii, J. Viinamaki, D. Torres Lobera, S. Valkealahti and T. Suntio, "Photovoltaic generator as an input source for power electronic converters," *IEEE Transactions on Power Electronics*, vol. 28, no. 6, pp. 3028-3038, June 2013.
[29] T. Suntio, J. Leppaaho, J. Huusari and L. Nousiainen, "Issues on solar-generator interfacing with current-fed MPP-tracking converters," *IEEE Transactions on Power Electronics*, vol. 25, no. 9, pp. 2409 - 2419, Sept 2010.
[30] F. Adamo, F. Attivissimo, A. Di Nisio and M. Spadavecchia, "Characterization and testing of a tool for photovoltaic panel modeling," *IEEE Transactions on Instrumentation and Measurement*, vol. 60, no. 5, pp. 1613-1622, May 2011.
[31] M. Averbukh, S. Lineykin, and A. Kuperman, "Obtaining small photovoltaic array operational curves for arbitrary cell temperatures and solar irradiation densities from standard conditions data," *Progress in Photovoltaics: Research and Applications*, vol. 21, no. 5, pp. 1016 – 1024, 2013.
[32] S. Lineykin, M. Averbukh and A. Kuperman, "An improved approach to extract the single-diode equivalent circuit parameters of a photovoltaic cell/panel," *Renewable and Sustainable Energy Reviews*, vol. 30, pp. 282 – 289, Feb. 2014.